BIOCHEMISTRY
including biophysical chemistry & molecular biology

ARTICLE

pubs.acs.org/biochemistry

Thermodynamics and Solvent Effects on Substrate and Cofactor Binding in *Escherichia coli* Chromosomal Dihydrofolate Reductase

Jordan Grubbs, Sharghi Rahmanian, Alexa DeLuca, Chetan Padmashali, Michael Jackson, Michael R. Duff, Jr., and Elizabeth E. Howell*

Department of Biochemistry and Cellular and Molecular Biology, University of Tennessee, Knoxville, Tennessee 37996-0840, United States

Supporting Information

ABSTRACT: Chromosomal dihydrofolate reductase from *Escherichia coli* catalyzes the reduction of dihydrofolate to tetrahydrofolate using NADPH as a cofactor. The thermodynamics of ligand binding were examined using an isothermal titration calorimetry approach. Using buffers with different heats of ionization, zero to a small, fractional proton release was observed for dihydrofolate binding, while a proton was released upon $NADP^+$ binding. The role of water in binding was additionally monitored using a number of different osmolytes. Binding of $NADP^+$ is accompanied by the net release of ~5−24 water molecules, with a dependence on the identity of the osmolyte. In contrast, binding of dihydrofolate is weakened in the presence of osmolytes, consistent with "water uptake". Different effects are observed depending on the identity of the osmolyte. The net uptake of water upon dihydrofolate binding was previously observed in the nonhomologous R67-encoded dihydrofolate reductase (dfrB or type II enzyme) [Chopra, S., et al. (2008) *J. Biol. Chem. 283*, 4690−4698]. As R67 dihydrofolate reductase possesses a nonhomologous sequence and forms a tetrameric structure with a single active site pore, the observation of weaker DHF binding in the presence of osmolytes in both enzymes implicates cosolvent effects on free dihydrofolate. Consistent with this analysis, stopped flow experiments find betaine mostly affects DHF binding via changes in k_{on}, while betaine mostly affects NADPH binding via changes in k_{off}. Finally, nonadditive enthalpy terms when binary and ternary cofactor binding events are compared suggest the presence of long-lived conformational transitions that are not included in a simple thermodynamic cycle.

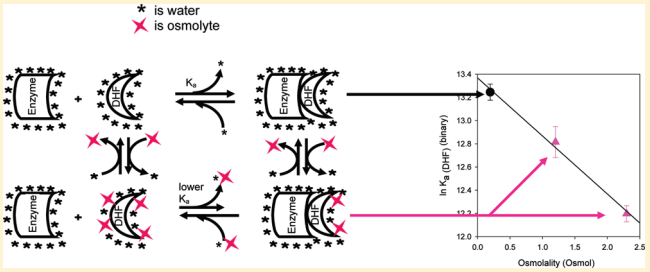

Chromosomal dihydrofolate reductase catalyzes the NADPH-dependent reduction of dihydrofolate (DHF) to tetrahydrofolate (THF). As this enzyme is the target for numerous drugs, including the antibacterial drug trimethoprim (TMP) and the anticancer drug methotrexate (MTX), it has been examined by nuclear magnetic resonance (NMR), crystallography, mutagenesis, stopped flow, molecular dynamics, and many other approaches for more than 30 years.[1−3] This study utilizes isothermal titration calorimetry (ITC) to probe binding in chromosomal DHFR from *Escherichia coli* (EcDHFR). Previous calorimetry approaches have focused on proton uptake associated with methotrexate binding to mammalian DHFRs[4,5] or used calorimetry to look at catalysis.[6,7] In addition, a recent calorimetry study of a nonhomologous, type II DHFR typified by R67 DHFR has proven to be helpful.[8]

Figure 1 compares the structures of EcDHFR and R67 DHFR. EcDHFR is a monomer with an eight-strand β-sheet core and four surrounding α-helices.[9] The basic structure consists of two rigid subdomains separated by a hinge region.[10] Ligand binding is accompanied by movement of the Met20 loop (residues 9−24).[3,11,12] The Met20 loop assumes a closed position in the productive catalytic complex as well as complexes in which the nicotinamide ring of the cofactor stacks favorably with the pteridine ring of the substrate as in the E·DHF·$NADP^+$ complex, where E is the enzyme (a list of the ligation states and corresponding loop positions is given in Table 1 of ref 13). The E·NADPH complex also displays a closed loop. In other complexes (such as E·DHF, E·folate, and E·THF complexes and various E·$NADP^+$·THF, E·THF, and E·NADPH·THF product complexes), the Met20 loop occupies an occluded position in the active site, displacing the nicotinamide ring of the cofactor outside of the binding pocket. Additional movement in the FG and GH loops (residues 119−132 and 142−150, respectively) also occurs upon binding. In contrast, R67 DHFR is a homotetramer possessing 222 symmetry, and the single active site pore can bind either two cofactors, two substrates, or one cofactor and one substrate.[14−16] These results, and a ternary complex crystal structure,[17] indicate NADPH and DHF occupy related sites. The latter is the productive complex. Few changes in the R67 structure occur upon ligand binding.[16−18]

Received: October 22, 2010
Revised: April 4, 2011
Published: April 04, 2011

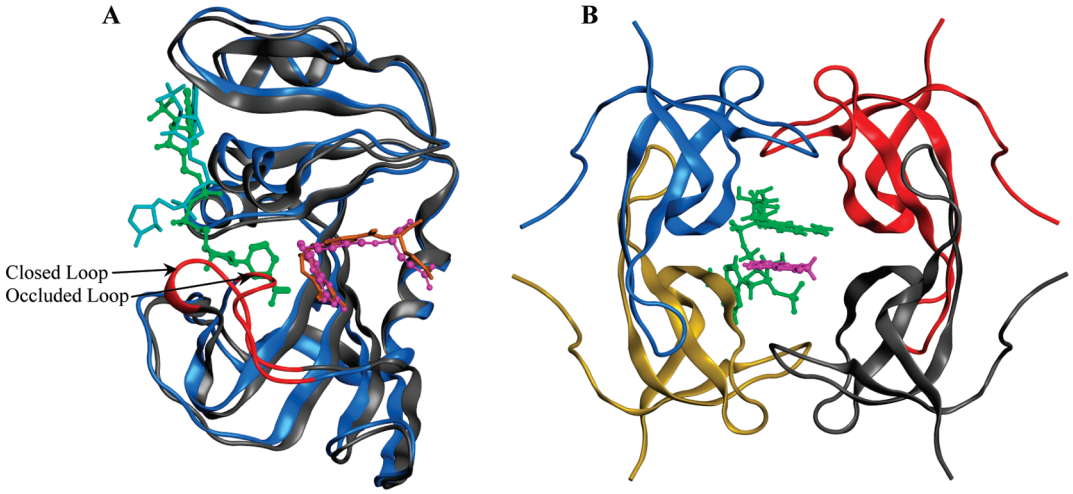

Figure 1. (A) Structure of PDB entry 1RX4 (occluded loop) overlaid with the structure of PDB entry 1RX2 (closed loop).[3] The 1RX4 structure is colored blue with bound dideazafolate and $NADP^+$ colored orange and cyan, respectively. The 1RX2 structure is colored black with bound folate and $NADP^+$ colored magenta and green, respectively. The Met20 loop (residues 16−22) is colored red. In the occluded state, the Met20 loop protrudes into the binding site. (B) Structure of R67 DHFR (PDB entry 2RH2[17]). Each polypeptide chain in the homotetramer is colored differently. The central hole is the active site, and bound dihydrofolate and $NADP^+$ are colored magenta and green, respectively. The *p*-aminobenzoyl-glutamate tail of DHF is disordered.

For those readers interested in a further comparison of the two DHFRs, we have provided Table S1 in Supporting Information. In addition, a 2005 review compares and contrasts the properties of these two enzymes.[19] At this point, we note EcDHFR has been described as a very well evolved enzyme[20] while R67 has been proposed to be a primitive enzyme.[19,21,22] A list of traits that support the designation of R67 as a primitive enzyme is given in Table S2 of the Supporting Information.

This study uses ITC to focus on the role of water. If water is involved in a binding interaction, perturbation of water activity should alter binding. For example, shorter contact distances typically exclude water. In the binding of lac repressor to DNA, Fried et al.[23] found increasing concentrations of ethylene glycol, betaine, and other osmolytes resulted in tighter binding. They interpreted this behavior as arising from dehydration of the protein−DNA interface, which led to tighter binding as water was released. This same type of behavior has been observed in R67 DHFR, as tighter binding of NADPH was observed upon addition of an osmolyte.[8] For the latter interaction, all osmolytes tested showed similar results, consistent with preferential exclusion of the solutes from the protein surface.[24−26]

For DHF binding to R67 DHFR, the opposite behavior has been observed, i.e., weaker substrate binding with increasing osmolyte concentrations, suggesting water stabilizes DHF binding. This unusual observation is typically taken to describe water uptake upon ligand binding and often is associated with conformational changes.[23,27,28] Weaker binding of a ligand in the presence of osmolytes can be achieved by either destabilization of the enzyme·ligand complex or stabilization of the free enzyme or the free ligand. For R67 DHFR, the same symmetry-related site binds either DHF with water uptake or a cofactor with water release. Because each site can bind either NADPH or DHF, we use binding of NADPH to R67 as an internal control; this suggests effects on the free enzyme or the enzyme·cofactor complex are unlikely as numerous osmolytes have the same effect, consistent with a preferential exclusion mechanism in which osmolytes are excluded from the protein surface.[24−26] Elimination of these options for DHF binding leaves effects of osmolytes on free DHF. A corollary of the hypothesis that DHF has differential interactions with water and osmolytes is that related osmolyte effects should then be observed in both R67 and *E. coli* chromosomal DHFRs.

With these studies as background, we began experiments to probe the role of water in DHF binding to EcDHFR, using osmolytes with different properties to determine if the primary effect was due to water or some other variable. To provide a complete picture of ligand binding, we additionally monitored the effects of osmolytes on the interaction of $NADP^+$ with EcDHFR. Using various osmolytes, this study finds water release accompanies $NADP^+$ binding, while weaker binding of DHF occurs in the presence of osmolytes.

MATERIALS AND METHODS

Protein Expression and Purification. A synthetic gene for EcDHFR was synthesized by Genscript and cloned into the pJET1.2 vector. The mutant (up) promoter sequence from Flensburg and Skold was used,[29] and codons for a GGGGHHHHHH sequence were added to the end of the gene to allow addition of a His tag sequence. High yields of wild-type (wt) DHFR were obtained when expressed in *E. coli* DH5α. Protein was purified using a nickel-NTA column (Invitrogen), followed by a methotrexate (MTX) affinity column (Sigma Chemicals). Elution of wt EcDHFR from the MTX affinity column required addition of folate, which was subsequently removed with a DEAE column.[30] Purified protein was dialyzed against distilled, deionized H_2O and then lyophilized. Protein concentrations were determined with a BCA (Pierce) assay.

Isothermal Titration Calorimetry. Affinities, stoichiometries, and ΔH values associated with binding were determined using isothermal titration calorimetry (ITC) as previously described.[14] At least two replicate titrations for each condition were performed using a VP-ITC microcalorimeter from MicroCal; 180−240 s was allowed after each injection for baseline equilibration.

DHFR concentrations ranged from 8.5 to 20 μM. The initial buffer used was MTA polybuffer (pH 7); it contained 50 mM MES, 100 mM Tris, and 50 mM acetic acid and maintains a constant ionic strength ($\mu = 0.1$) from pH 4.5 to 9.5.[31] All buffers contained 1 mM EDTA and 5 mM β-mercaptoethanol. For titrations with an osmolyte present, MTA buffer with osmolyte was used in the reference cell. The "c value" ($=[P]_{total}/K_d$) ranged from 1 to 68, within the suggested range of 1−1000.[32]

Origin version 7 and SEDPHAT[33] were used to analyze the ITC data. Export of Origin fits into SEDPHAT allows global fitting of replicate data sets. These fits used the single-site model (A + B ↔ AB). Errors were calculated using the Monte Carlo for nonlinear regression option.

In ITC, the enthalpic signal describes all the components involved in the binding process, including any effects associated with proton release (or uptake). To determine whether proton release or uptake occurs, binding was performed in various buffers, which possess different heats of ionization and protonation. If no proton release or uptake occurs, the observed enthalpy value remains constant. However, if binding is coupled to perturbation of a pK_a, such that proton release or uptake occurs, then the observed enthalpy signal varies according to the following equation:

$$\Delta H_{observed} = \Delta H_{binding} + n\Delta H_{protonation} \quad (1)$$

where $\Delta H_{observed}$ is the observed enthalpy change upon binding of ligand to enzyme, $\Delta H_{protonation}$ is the protonation enthalpy of the buffer (same pH and temperature), and n is the number of protons transferred upon ligand binding.[34] To assess proton uptake and release upon ligand binding in EcDHFR, ITC titrations were performed in several buffers. The additional buffers were 100 mM MOPS with 31 mM NaCl; 100 mM HEPES with 62 mM NaCl; another polybuffer consisting of 33 mM succinic acid, 44 mM imidazole, and 44 mM diethanolamine (SID); and 47 mM potassium phosphate buffer. The same pH and ionic strength (μ) that were used for the MTA buffer (pH 7.0, $\mu = 0.1$) were maintained. Heats of ionization and protonation for the buffers were determined in separate ITC experiments as described by Jelesarov and Bosshard.[35] Briefly, a 5 mM solution of HCl was titrated into the sample cell containing buffer. Ten injections (5 μL) allowed measurement of an average enthalpy change. A control titration injected distilled, deionized H_2O into buffer to correct for the heat of dilution. The following enthalpy changes were measured at 25 °C and pH 7: −7.28 ± 0.01 kcal/mol for SID, −6.97 ± 0.01 kcal/mol for MTA, −4.59 ± 0.01 kcal/mol for MOPS with NaCl, −4.23 ± 0.01 kcal/mol for Hepes with NaCl, and −1.01 ± 0.01 kcal/mol for phosphate. The values for Hepes, MOPS, and phosphate are similar to those previously measured.[34]

Water Activity Measurements. A Wescor 5500 vapor pressure osmometer was used to obtain the osmolality of the solutions. This value was converted into water activity using the equation

$$a_{H_2O} = e^{-0.018 \times \text{osmolality}} \quad (2)$$

where a_{H_2O} is the water activity.[36]

The binding of ligand, for example, DHF, to EcDHFR in a buffer containing neutral osmolytes (S) can be described by

$$\text{DHF} + \text{EcDHFR} \rightleftarrows \text{EcDHFR}\cdot\text{DHF} + \nu_{H_2O}H_2O + \nu_S S \quad (3)$$

where ν_{H_2O} and ν_S are the stoichiometric coefficients of water and the osmolyte, respectively. From the work of Wyman,[37] ln K_a can be related to ln a_{H_2O} according to

$$\frac{\partial(\ln K_a)}{\partial(\ln a_{H_2O})} = \nu_{H_2O} + \nu_S\left[\frac{\partial(\ln a_S)}{\partial(\ln a_{H_2O})}\right] \quad (4)$$

Various groups have found that low-molecular weight osmolytes are preferentially excluded from the surface of proteins.[24−26] This observation suggests that the value of ν_{H_2O} would predominate over ν_S in eq 4. This prediction can be tested by using osmolytes from different classes, which differentially associate with proteins (and presumably ligands as well[24,25]).

Rapid Kinetics. Stopped flow experiments at room temperature (20.5 °C) were performed on a model SX20 Applied PhotoPhysics system with a dead time of 1 ms. For NADPH binding, the samples were excited at 290 nm and a 455 nm filter was used to monitor the transfer of energy from the enzyme to cofactor. Enzyme and ligand were mixed, and the resulting data were fit using Pro-Data SX. Two phases were observed; 5−20 traces of the fast phase (2−200 ms time interval) were fit to a single exponential with a linear rate:

$$F(t) = A\exp(-k_{app}t) + k_a t + B \quad (5)$$

where $F(t)$ is the fluorescence intensity as a function of time, A is the amplitude of the quench, k_{app} and k_a are the exponential and linear rates, respectively, and B is the final fluorescence. The linear rate corrects for the small contribution of the slow rate on the fast time scale. The slow phase was observed from 200 ms to 200 s, and the data were fit to a single exponential. The final protein concentration was 0.5 μM, and NADPH concentrations varied from 0.125 to 2 μM.

For DHF binding, quenching of tryptophan fluorescence (excitation at 280 nm) using a 320 nm cutoff filter was monitored. The final protein concentration was 0.4 μM, while DHF concentrations varied from 0.15 to 4.8 μM. The fast phase was treated as described above. For the slow phase, an upward, linear slope was also present and appeared to be associated with some DHF process, possibly photobleaching[38] or photolysis.[39] The origin of the slope was identified by observation of a similar trend for mixing DHF with buffer. To correct for this effect, we subtracted the kinetic trace from the DHF control from the DHF−enzyme slow phase. However, this correction appeared to be inconsistent as sometimes a slope remained. Therefore, analysis of the slow phase was not pursued.

Cayley et al.[40] proposed a model describing the observed biphasic binding data. In this model, two interconvertible conformations of DHFR exist (E_1 and E_2); however, ligand (L) binds to only one of these forms (E_l) with high affinity.

$$E_2 \leftrightarrow E_1 + L \leftrightarrow E_1\cdot L \quad (6)$$

The fast phase describes binding of ligand to E_1 and the slow phase the interconversion of E_2 to E_l with subsequent binding of ligand to E_1. If binding of ligand to E_1 is a simple bimolecular process, then the observed rate constant for the fast phase quench can be described by

$$k_{app} = k_{on}[\text{ligand}] + k_{off} \quad (7)$$

where k_{on} and k_{off} are the association and dissociation rate constants, respectively.[38,40,41]

A second, independent method for determining k_{off} uses a competition approach. Here, when dissociation of an enzyme·

Table 1. Thermodynamic Parameters Associated with Formation of Binary and Ternary Complexes in MTA Buffer at pH 7, 25 °C, and μ = 0.1[a]

complex	K_d (μM)	ΔG (kcal/mol)	ΔH_{obs} (kcal/mol)	$T\Delta S$ (kcal/mol)	n
DHF binding to EcDHFR	1.77 ± 0.13	−7.84	−10.5 ± 0.3	−2.67	0.94 ± 0.01
folate binding to EcDHFR	4.72 ± 0.50	−7.26	−11.7 ± 0.8	−4.43	0.81 ± 0.03
NADPH binding to EcDHFR	0.195 ± 0.013	−9.15	−22.5 ± 0.2	−13.39	0.94 ± 0.01
$NADP^+$ binding to EcDHFR	3.09 ± 0.10	−7.51	−20.7 ± 0.3	−13.19	0.85 ± 0.01
DHF binding to EcDHFR·$NADP^+$	0.177 ± 0.013	−9.20	−8.50 ± 0.08	0.70	1.17 ± 0.01
$NADP^+$ binding to EcDHFR·DHF	1.38 ± 0.07	−7.99	−12.2 ± 0.2	−4.20	0.93 ± 0.01

[a] Global fits of two to three data sets to a single-site model (A + B ↔ AB) were analyzed using SEDPHAT. The Gibbs free energy values were calculated from the equation $\Delta G = -RT \ln K_d$, and $T\Delta S$ values were obtained from the relationship $\Delta G = \Delta H - T\Delta S$.

first ligand complex occurs in the presence of an excess of a second ligand, formation of the enzyme·second ligand complex occurs. If the fluorescence signal is different between the two complexes, k_{off} for the first ligand can be monitored. For competition experiments with DHF, the EcDHFR·DHF complex (2 μM enzyme preincubated for 20 min with 22 μM DHF) was mixed with a large excess of methotrexate (0.05−0.2 mM). For cofactor competition experiments, fluorescence energy transfer was used. When NADPH dissociates from the enzyme·NADPH complex (2 μM DHFR and 20 μM NADPH), excess $NADP^+$ (0.1−0.5 mM) binds to free enzyme, and the loss of energy transfer describes k_{off} for NADPH. These experiments assume k_{off}(first ligand) ≪ k_{on}(second ligand) × [second ligand] ≫ k_{on}(first ligand) × [first ligand]. These conditions were confirmed by altering either methotrexate or $NADP^+$ concentrations, which did not affect the observed rate.

RESULTS

Initial Binding Experiments. ITC experiments allow measurement of binding affinities, stoichiometries, and enthalpies. The results from our initial titrations are listed in Table 1. A sample titration and a sample global fit using SEDPHAT[33] are shown in Figure S1 of the Supporting Information. Comparison of the K_d values obtained in this study with previously published values shows up to 8-fold differences, which may be due to the changes in buffer, ionic strength, pH, and/or our use of a His-tagged DHFR. For example, our K_d values for folate, DHF, $NADP^+$, and NADPH binding to the apoenzyme are 4.7 ± 0.5, 1.8 ± 0.1, 3.1 ± 0.1, and 0.20 ± 0.01 μM, respectively. For comparison, the Benkovic lab reports values of 1.0 ± 0.1, 0.22 ± 0.06, 24 ± 4, and 0.33 ± 0.06 μM for binding of folate, DHF, $NADP^+$, and NADPH, respectively [determined by fluorescence quenching at pH 6 in 50 mM MES, 25 mM Tris, 25 mM ethanolamine, and 100 mM sodium chloride buffer (μ = 0.15)[38,42]].

Ternary complex formation was additionally monitored (Table 1). Our ITC values indicate ∼10-fold tighter binding of DHF to the enzyme·$NADP^+$ complex and ∼2-fold tighter binding of $NADP^+$ to the enzyme·DHF complex compared to binding of the ligands to the apoenzyme. For comparison, literature values from the Benkovic group (obtained at pH 6 using stopped flow and calculated as k_{off}/k_{on} rates) are 0.43 μM for DHF binding to the E·$NADP^+$ complex and 11.6 μM for $NADP^+$ binding to the EcDHFR·DHF complex. Other groups have also noted cooperativity between the cofactor and various folates.[10,40]

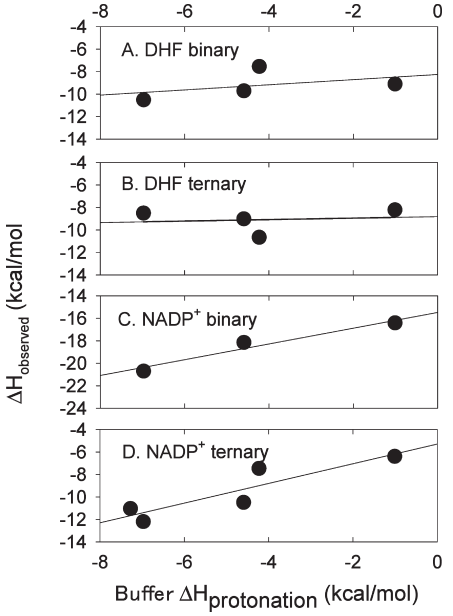

Figure 2. Plot of the heat of buffer protonation vs $\Delta H_{observed}$. Three to five different buffers were used in these experiments. Values from the ITC fits are given in Tables S3 and S4 of the Supporting Information. Panel A shows the results for binding of DHF to apo EcDHFR. Panel B presents the data for formation of the DHF ternary complex. Panel C depicts the data for the $NADP^+$ binary complex interaction, while panel D shows the pattern associated with formation of the $NADP^+$ ternary complex. All slopes are positive, consistent with proton release. Values for the fits to eq 1 are listed in Table 2.

Effects of Protonation on Ligand Binding. Numerous studies have found protonation events accompany binding of DHF to EcDHFR;[43−50] thus, complex formation was studied in several buffers possessing different heats of ionization. Also, binding of cofactor may involve pK_a perturbations as well.[51] Tables S3 and S4 of the Supporting Information list the fit values for the various titrations, and Figure 2 plots the heat of buffer protonation versus the observed enthalpy. Using eq 1, the binding enthalpy and n, the level of proton uptake or release, can be extracted. As listed in Table 2, the slopes for binding of DHF to either the apoenzyme or the enzyme·$NADP^+$ complex are small and within error of each other, consistent with either no or partial release of protons to the buffer upon complex formation. The slope for binding of folate to the apoenzyme is slightly higher, but still within error of the DHF value. We also note these are net values and could include contributions from either the

Table 2. Effects of Protonation on Ligand Binding[a]

complex	no. of protons	$\Delta H_{binding}$
DHF binding to EcDHFR	0.23 ± 0.32 (release)	−8.26 ± 1.53
DHF binding to EcDHFR·NADP$^+$	0.07 ± 0.3 (release)	−8.82 ± 1.46
folate binding to EcDHFR	0.51 ± 0.36	−6.92 ± 1.68
NADP$^+$ binding to EcDHFR	0.70 ± 0.16	−15.5 ± 0.78
NADP$^+$ binding to EcDHFR·DHF	0.87 ± 0.25	−5.30 ± 1.33
NADPH binding to EcDHFR	0.89 ± 0.56	−14.7 ± 2.6

[a] Binding was monitored in three to five buffers at pH 7 possessing different heats of ionization. Tables S3 and S4 of the Supporting Information list all the values obtained from fitting the titrations. Figure 2 plots $\Delta H_{protonation}$ vs $\Delta H_{observed}$ for several binary and ternary complex formation experiments. The slopes in these plots correspond to the number of protons taken up or released, while the *y*-intercept corresponds to the ΔH associated with binding.

ligand and/or protein. For NADP$^+$ binding, the slopes are more obvious, with the net release of ~0.7−0.9 proton to the buffer. A similar slope is observed for NADPH binding.

Role of Water in Ligand Binding. Ligand binding can also be probed by addition of varying osmolytes. This approach monitors any change in the number of water and/or solute molecules associated with the initial and final states.[23,36,52−55] Addition of an osmolyte can, however, alter the solvent dielectric constant or volume exclusion, which can also affect binding. To parse out these effects, we used osmolytes with different characteristics. For example, while sucrose and glycine betaine both affect water activity, they provide opposite effects on the dielectric constant of the solution.[23,56,57] If both compounds show similar results in osmolality plots, then effects on the dielectric constant are not involved. To test the role of volume exclusion on binding, PEGs of increasing size are typically used. The osmotically active volume is the volume accessible to water but inaccessible to osmolyte, for example, active site clefts. The osmotically active volume depends on the size of the osmolyte, with larger osmolytes detecting changes in larger volumes. Osmotic stress occurs as the solution compensates for this exclusion.[23,52] A last possibility is direct interaction of the osmolyte with either the ligand or protein.[58,59] If similar results are observed with chemically different osmolytes, the last option is unlikely.[24,25]

With this background in mind, binding of DHF to the EcDHFR·NADP$^+$ complex was monitored in the presence of the neutral osmolytes glycerol, ethylene glycol, trimethylamine *N*-oxide (TMAO), dimethyl sulfoxide (DMSO), glycine betaine, sucrose, and polyethylene glycol (PEG) 400. If a linear relationship is observed in plots of osmolality versus ln K_a, then effects on water are involved.[23,59−61] Figure 3A shows the linear relationships associated with plots of osmolality versus ln $K_{a(DHF)}$. As a precaution, we also plotted effects on solution dielectric, and overlapping data were not observed (see Figure S2 of the Supporting Information). In addition, Table S5 and Figure S3 of the Supporting Information give the volume exclusion data for formation of the ternary DHF complex in the presence of nine osmolytes, including PEG 3350 and PEG 8000. When the higher-molecular weight PEGs are used to probe binding, the Δn_w values increase, consistent with their probing larger surface features as the osmolyte becomes too large to fit in the active site. However, there is no evidence of volume exclusion with the non-PEG osmolytes.

From eqs 2 and 4, the slope of a plot of osmolality versus ln $K_{a(DHF)}$ is a function of the change in the number of water

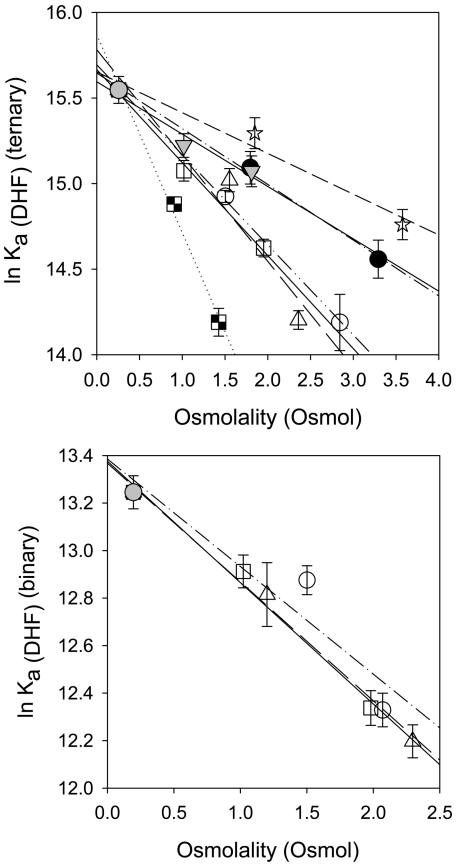

Figure 3. Plot of ln K_a values for DHF vs osmolality. The top panel contains data for DHF binding to the EcDHFR·NADP$^+$ complex, while the bottom panel shows DHF binding to the apoenzyme. Data for buffer (gray circles), glycerol (●), ethylene glycol (☆), TMAO (gray triangles), sucrose (□), DMSO (○), glycine betaine (△), and PEG 400 (black and white squares) are shown. Slopes for these plots were converted to Δn_w using the relationship d(ln K_a)/d(osmolality) = $-\Delta n_w/55.6$, and the values are listed in Table 3.

molecules, Δn_W, involved in binding of DHF to the EcDHFR·NADP$^+$ complex. The slopes associated with the individual osmolytes were converted to n_W values, which are listed in Table 3. The Δn_W values vary from 13 to 64. Variable slopes are common in osmolality studies, but their origin is not clear.[58,59,61−74] What is interesting and unusual is that the K_a decreases (or K_d increases) upon addition of osmolyte. This is the same result observed in R67 DHFR (also shown in Table 3[8]). Because R67 DHFR possesses a totally different sequence and structure, the convergence of these two results implicates effects of osmolytes on free DHF. In other words, what is similar in the E·NADP$^+$ + DHF ↔ E·NADP$^+$·DHF binding mechanism (where E is enzyme) for R67 DHFR and EcDHFR is the free DHF species. For "water uptake" to occur in both DHFRs, effects of osmolytes on free DHF are likely involved.

A more limited set of osmolytes was used to analyze titration of DHF into apo EcDHFR. The three osmolytes showing the strongest effects in Figure 3A (betaine, sucrose, and DMSO) were selected for analysis. Figure 3B shows the results, and Table 3 lists the associated Δn_w values, which range from 25 to 28. From Table 3, these values are within error of those observed for formation of the ternary complex, indicating both binary binding and ternary binding of DHF are weakened in the presence of osmolytes.

Table 3. Δn_w Values Describing Binding of Ligands to EcDHFR[a]

osmolyte	Δn_w for DHF binding to EcDHFR·NADP$^+$	Δn_w for DHF binding to apo EcDHFR	Δn_w for NADP$^+$ binding to EcDHFR·DHF	Δn_w for NADP$^+$ binding to apo EcDHFR	Δn_w for DHF binding to R67 DHFR[b]
ethylene glycol	13 ± 1	–	−10 ± 3	–	25 ± 8
glycerol	18 ± 1	–	−5 ± 2	–	16 ± 3
TMAO	17 ± 4	–	−9 ± 6	–	22 ± 1
DMSO	29 ± 1	25 ± 9	−24 ± 3	−29 ± 5	41 ± 7
sucrose	30 ± 2	28 ± 3	−5 ± 4	18 ± 8	40 ± 4
glycine betaine	34 ± 9	28 ± 2	−14 ± 5	−10 ± 1	60 ± 13
PEG 400	64 ± 5	–	−47 ± 8	–	78 ± 11

[a] Tables S6−S9 of the Supporting Information list all the values obtained from fitting the titrations. The slopes from plots of osmolality vs ln K_a were used to calculate Δn_w values using the relationship d(ln K_a)/d(osmolality) = $-\Delta n_w/55.6$. A negative value indicates release of water upon ligand binding, while a positive value describes uptake of water upon ligand binding. [b] Data for nonhomologous R67 DHFR were measured by steady state kinetics [$k_{cat}/K_{m(DHF)}$].[8] ITC was used to monitor ligand binding in R67 DHFR for a subset of the osmolytes.[8]

Next, binding of NADP$^+$ to the EcDHFR·DHF complex was monitored in the presence of all seven osmolytes. A slope opposite to that observed for DHF binding was observed in Figure 4A, consistent with release of water upon cofactor binding. Δn_w values varied from −5 to −47 (see Table 3). Because each osmolyte has individual effects, this result suggests preferential osmolyte interaction with either protein and/or ligand.

Effects of osmolytes on binding of NADP$^+$ to the apoenzyme were analyzed, using a limited subset of osmolytes. Figure 4B shows the data describing betaine and DMSO effects, consistent with release of water upon cofactor binding. Table 3 lists the Δn_w values, which are within error of those observed for formation of the NADP$^+$ ternary complex. Surprisingly, addition of sucrose results in a positive Δn_W value, consistent with weaker binding of NADP$^+$. This Δn_W value is different from that seen for formation of the NADP$^+$ ternary complex. As betaine and sucrose have opposite effects here, it is possible in the sucrose experiments that some combination of water and/or dielectric effects could be occurring.

Finally, binding of NADPH to apo EcDHFR was monitored in the presence of increasing concentrations of betaine. Tighter binding of NADPH was observed as shown in Figure S4 of the Supporting Information, which plots ln K_a versus solution osmolality. Conversion of the slope to Δn_W indicates the release of −14 ± 3 water molecules.

The enthalpies associated with binding were additionally analyzed, and Figure S5 of the Supporting Information shows an enthalpy−entropy compensation plot. Because the thermodynamic parameters display a large range of ΔH values and the only components that vary are the water and osmolyte concentrations, these results imply that water-mediated enthalpy−entropy compensation is the mechanism by which changes in enthalpy occur.[75−78]

Stopped Flow Analysis. How does betaine affect K_d values? Does it affect k_{on} and/or k_{off} rates? To address these questions, we used a rapid kinetics approach. As a weak signal associated with NADP$^+$ binding kinetics caused inconsistent data fitting, NADPH binding was monitored instead. Figure S6 of the Supporting Information shows a set of sample data. Figure 5A shows the relationship between the NADPH concentration and the observed rate for the fast phase describing binding of NADPH to the E_1 conformer (eq 6). Previous stopped flow experiments proposed that at high cofactor concentrations (~10 μM), NADPH

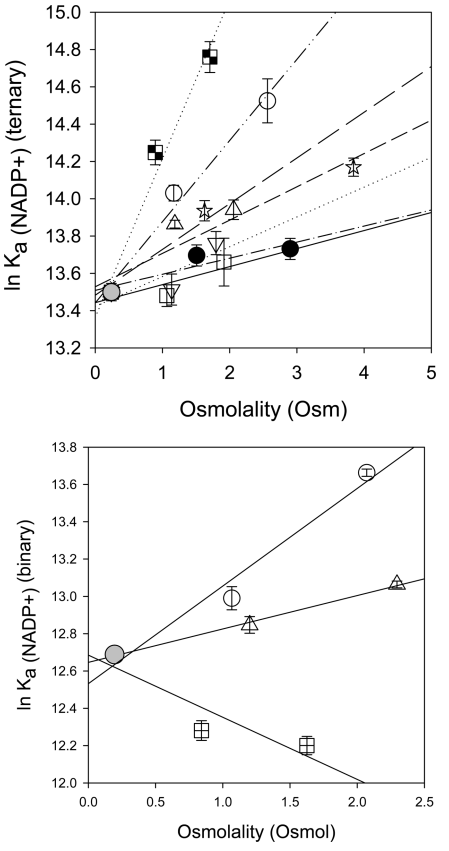

Figure 4. Plot of ln K_a values for NADP$^+$ vs osmolality. The top panel shows data for NADP$^+$ binding to the DHFR·DHF complex, while the bottom panel shows data for NADP$^+$ binding to the apoenzyme. Data for buffer (gray circles), glycerol (●), ethylene glycol (☆), TMAO (▽), sucrose (□), DMSO (○), glycine betaine (△), and PEG 400 (black and white squares) are shown. Slopes for these plots were converted to Δn_w using the relationship d(ln K_a)/d(osmolality) = $-\Delta n_w/55.6$, and the values are listed in Table 3.

can also bind to the E_2 conformer and this step can be included by fitting to a double-exponential equation.[79,80] Fitting our cofactor binding data to a double-exponential model did not significantly improve the quality of the fit; thus, a single exponential with a linear rate fit was used to fit the fast phase kinetic data. The k_{on} and k_{off} values were determined with eq 7 and are listed in Table 4.

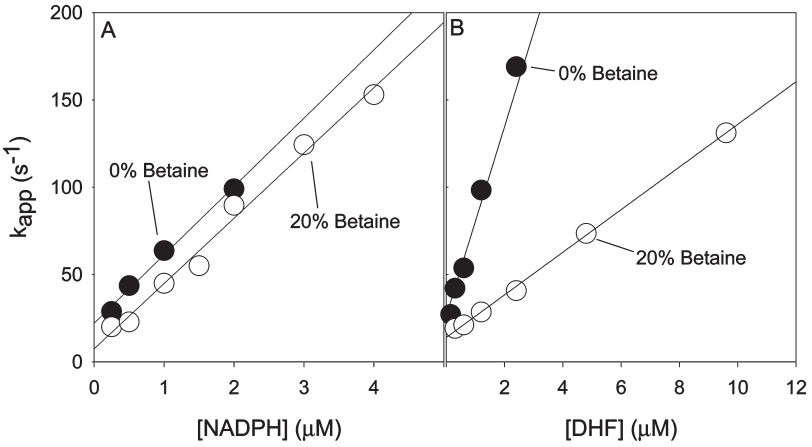

Figure 5. Stopped flow analysis of ligand binding. Panel A plots the rates for the fast phase of binding of NADPH to EcDHFR in MTA buffer (pH 7.0) containing either 0 (●) or 20% (○) betaine (w/v) vs ligand concentration. Panel B shows the results for binding of DHF to EcDHFR in MTA buffer (pH 7.0) containing either 0 (●) or 20% (○) betaine (w/v). The plots were used to calculate k_{on} and k_{off} according to eq 7, and the data are listed in Table 4.

Table 4. Rate Constants for DHF and NADPH Binding As Monitored by Stopped Flow in MTA Buffer with 0 and 20% Betaine

ligand	[betaine] (w/v)	k_{on} (M^{-1} s^{-1})[a]	k_{off} (s^{-1})[a]	k_{off} (s^{-1})[b]	osmolality (osmolal)
NADPH	0%	$(3.9 \pm 0.2) \times 10^7$	22.7 ± 2.8	3.3 ± 0.2	0.2
NADPH	20%	$(3.7 \pm 0.2) \times 10^7$	7.4 ± 3.9	1.0 ± 0.1	2.3
DHF	0%	$(6.3 \pm 0.2) \times 10^7$	19.8 ± 2.6	13.6 ± 1.0	0.2
DHF	20%	$(1.2 \pm 0.2) \times 10^7$	13.9 ± 0.9	9.1 ± 0.5	2.3

[a] Determined from a plot of k_{obs} vs ligand concentration. [b] Determined from a competition assay against $NADP^+$ for NADPH or methotrexate for DHF.

A second fluorescent phase was observed beyond 0.2 s, describing conversion of E_2 to E_1, with subsequent binding of a cofactor. The rate of conversion of enzyme from E_2 to E_1 was measured and found to be cofactor-independent and equal to 0.027 ± 0.005 s^{-1}. This rate agrees with the value observed by Cayley et al.[40] The amplitudes of the first, fast kinetic phase and the second, slow phase were used to determine the ratio of E_1 to E_2. For all NADPH concentrations, similar ratios of 0.94 ± 0.11 were obtained, in agreement with previously published values for the relative concentrations of the two conformers.[38,40]

Using these kinetic data, the overall NADPH dissociation constant can be calculated using eq 8:

$$K_d = k_{off}/k_{on} \times [(K_{eq} + 1)/K_{eq}] \quad (8)$$

where K_{eq} is the equilibrium constant for the conversion of the enzyme between the E_1 and E_2 conformers.[38] A K_d of 1.14 ± 0.11 μM was calculated for the binding of the cofactor to the enzyme. This is approximately 6-fold higher than the value determined via ITC (see Table 1).

As binding of a ligand to EcDHFR has sometimes been described as an isomerization process,[38,79,81] we additionally monitored k_{off} using a competition method. For cofactors, k_{off} for the EcDHFR·NADPH complex was determined through competition with $NADP^+$. Using this approach, k_{off} (Table 4) was found to be almost 7 times lower than the k_{off} determined from the relaxation experiments or k_{app} (Figure 5A). Discrepancies in k_{off} values determined by the two approaches have been noted previously for binding of cofactors to EcDHFR.[79,81] When the k_{off} from the competition assay was used to determine K_d, a value of 0.17 μM was obtained, which agrees well with our ITC data This suggests that either the k_{off} determined from the competition assay is more accurate than that determined from the plot of k_{app} versus cofactor concentration, which has been suggested by Dunn et al.,[79] or a conformational change between the EcDHFR·NADPH complex and the EcDHFR*·NADPH complex occurs (where the asterisk denotes a different conformation).

The binding study described above was repeated in 20% betaine, and the k_{app} rates were found to be slower (Figure 5A). While k_{on} was unperturbed by the presence of betaine, k_{off} decreased ~3-fold (Table 4). The rate associated with the slow phase did not change appreciably in the presence of betaine, with a rate of 0.031 ± 0.004 s^{-1}. The ratio of the amplitudes of the fast and slow kinetic processes for binding of NADPH to the enzyme in the presence of 20% betaine was 1.00 ± 0.11 (corresponding to the E_1:E_2 ratio). Similar E_1:E_2 ratios in the absence and presence of betaine suggest that betaine does not affect the equilibrium between the two enzyme conformers.

The competition assay was repeated to measure k_{off} for NADPH in the presence of 20% betaine, and the k_{off} was ~7-fold smaller than the k_{off} determined in the relaxation experiments (see Table 4). In addition, k_{off} was 3-fold lower in the presence of betaine than in just MTA buffer. The overall dissociation constant was determined from the rate constants for NADPH in the presence of betaine (eq 8) and was 0.052 ± 0.005 μM using the k_{off} determined from the competition assay. The enzyme's affinity for NADPH increased approximately 3-fold in the presence of betaine. For comparison, the ITC studies found betaine tightened the binding affinity for NADPH by a factor of 1.7 (Table S10 of the Supporting Information).

The binding of DHF to EcDHFR was also monitored using stopped flow kinetics as shown in Figure 5B. Values for k_{on} and k_{off} were obtained from fitting the data to eq 7 and are listed in Table 4. The k_{off} values from the relaxation (k_{app}) and

competition assays were relatively close and are comparable to those of Fierke et al.[38] A K_d of 0.63 ± 0.07 μM for DHF was calculated using eq 8, assuming a 1:1 E_1:E_2 conformer ratio as determined from the NADPH binding studies. This is an approximately 3-fold tighter affinity than the one determined from ITC (see Tables 1 and 4). The second phase of DHF binding was not analyzed because of the difficulty in correcting for the baseline slope.

The DHF binding experiments described above were repeated in MTA buffer containing 20% betaine. An obvious result is a large decrease in the observed rate. Figure 5B shows the observed rates as the DHF concentration is varied, and Table 4 gives the k_{on} and k_{off} values. A 5-fold decrease in k_{on} and a 1.4-fold decrease in k_{off} are observed when results in MTA versus those in MTA and 20% betaine buffer are compared. The DHF k_{off} was also measured in the competition assay and was found to be comparable to the k_{off} obtained from the relaxation approach (Table 4). We estimated the DHF K_d using eq 8 and the 1:1 E_1:E_2 conformer ratio from our NADPH data; the resulting K_d was 2.28 ± 0.11 μM, indicating ~3-fold weaker binding of DHF in the presence of betaine. These stopped flow results indicate addition of betaine weakens binding for DHF, consistent with our ITC results. We find effects of betaine on DHF binding mostly arise from changes in k_{on}, while the effects of betaine on NADPH binding mostly arise from changes in k_{off}.

Circular Dichroism. To monitor the effect of cosolvents on the secondary structure of apo EcDHFR, we monitored the CD signal. Experimental details are given in the legend of Figure S7 of the Supporting Information. The spectra in this figure show no significant change upon addition of either 1.5 M sucrose, 15% TMAO, 20% glycerol, or 30% PEG 400. Loveridge et al.[82] also found no large changes in the CD signal occur in EcDHFR upon addition of 50% cosolvent, including ethylene glycol, glycerol, sucrose, methanol, and ethanol.

DISCUSSION

The ITC signal contains information describing a number of processes, including the binding enthalpy, effects due to perturbation of pK_a values, any contributions to ΔH associated with conformational changes, and effects on water structure. To deconvolute ionization effects, we use buffers with different heats of ionization.[35,83,84] To monitor the role of water, we add neutral osmolytes to the buffer. To tackle conformational changes, we compare enthalpies for the two pathways to formation of the ternary complex.

Protonation Effects. Previous calorimetry studies of chromosomal DHFRs have focused on mammalian variants. In their study of chicken liver DHFR, Subramanian and Kaufman found enthalpy-driven binding for folate, DHF, and methotrexate, while binding of NADPH and $NADP^+$ was mostly entropy-driven.[4] They also found that DHF and folate bound with no proton uptake while NADPH binding was accompanied by a fractional release of a proton from the coenzyme. Similar results were also seen by Gilli et al.[5] in their study of bovine liver DHFR.

Our study finds that both DHF and cofactor binding events are enthalpy-driven. In addition, our results agree with the previous protonation results; there is no net protonation upon DHF binding, while there is a net fractional deprotonation upon cofactor binding. While the latter may correspond to alteration of one of the phosphate pK_a values upon cofactor binding,[51,85] it could also describe concurrent pK_a perturbation events in the protein.

A second parameter that can be obtained from protonation effects is $\Delta H_{binding}$ (see Table 2). For DHF, the values for formation of binary and ternary complexes are within error of each other. In contrast, there is an ~10 kcal/mol difference between binary and ternary $NADP^+$ binding events. This enthalpic difference probably does not report on either protonation or solvation differences as the data in Tables 2 and 3 suggest similar proton release and Δn_w values for formation of binary and ternary complexes. This issue will be continued in Thermodynamic Cycle Analysis.

Osmolyte Effects. Different osmolytes have different effects on binding of both cofactor and substrate. These results can be explained by several potential scenarios. The first possibility is that the different slopes in Figures 3 and 4 arise from preferential binding of the osmolyte to the protein, ligand, and/or protein−ligand complex.[58,62] This is the most likely scenario as osmolytes will compete with water to fill the hydration shell surrounding these molecules. (Solvent accessible area calculations addressing this issue have been performed and are provided as Supporting Information.)

A second option for explaining the variable slopes in Figures 3 and 4 is the fact that conformational changes occur upon ligand binding. For DHF binding, if these changes result in an increased surface area, then release of water upon ligand binding could be masked by the water uptake associated with the conformational change. Examples of this phenomenon include binding of glucose to hexokinase,[27] aspartate to ATCase,[28] DNA to repressors,[23] etc. While conformational changes have been observed in EcDHFR using stopped flow fluorescence,[38,40,80,86] differences in crystal structures,[3] and many NMR studies,[11−13,87,88] they have been linked to different ligation states rather than increases in ionic strength or osmolality. To address the possibility of conformational change, we note addition of 20% betaine does not alter the E_1 to E_2 conformational transition, as probed by stopped flow. Further, the CD spectra in Figure S7 of the Supporting Information do not suggest significant secondary structure changes occur in apo EcDHFR upon addition of TMAO, glycerol, sucrose, or PEG 400. We also note 27 different EcDHFR crystal structures (including apo, folate binary, $NADP^+$ binary, folate and $NADP^+$ ternary, and dideazatetrahydrofolate and $NADP^+$ ternary) have been obtained using 9−30% PEG 6000 as a precipitating agent.[3] DHFR from *Staphylococcus aureus* has been crystallized using 6.5% PEG 3350 as a precipitating agent and X-ray data collected with 20% ethylene glycol as a cryoprotectant.[89] Mouse DHFR structures have been obtained using 20% PEG 4000 as a precipitating agent and 15% glycerol as a cryoprotectant.[90] These concentrations are within the range used in our study. Because solution NMR structures closely approximate those obtained by X-ray crystallography,[13] it seems likely that cosolvent addition does not greatly alter the conformational landscape.

To return to the preferential binding model, we consider weaker binding of DHF upon addition of osmolytes, consistent with water uptake. Because water uptake upon ligand binding is unusual,[91−93] and as this behavior is observed for DHF binding in two quite different DHFR scaffolds, it seems likely that osmolytes affect free DHF. (NADPH binding served as an internal control in R67 DHFR as a single slope was observed in plots of ln K_a versus osmolality. Because DHF and NADPH share symmetry-related sites in R67, this observation makes the binding of osmolytes to the R67 protein unlikely, leaving DHF as the target for osmolyte interaction.[8]) There are several possibilities for explaining weaker binding of DHF to EcDHFR in the

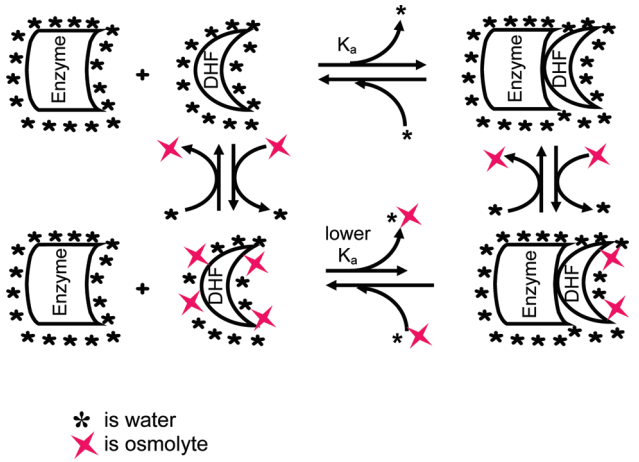

Figure 6. Cartoon depicting preferential interaction of osmolytes with free DHF. In the absence of osmolytes, DHF binds to either EcDHFR or R67 DHFR and water is released. Added osmolytes interact weakly with DHF. For DHF to bind to DHFR, both osmolytes and water must be released. The more tightly bound osmolytes would have stronger effects on the DHF K_a, while the more weakly bound osmolytes would have weaker effects. (This model does not exclude the possible binding of osmolytes to EcDHFR, which could describe the differing effects of osmolytes on $NADP^+$ binding.)

presence of osmolytes. The first model proposes that osmolytes tighten the dimerization constant of DHF, which is 38.5 mM.[94] In this model, addition of an osmolyte would increase the concentration of DHF dimers, so for DHF to bind EcDHFR, it would first need to dissociate into monomers,[95] requiring water uptake at the DHF dimer interface. On the basis of solvent accessible area calculations (provided as Supporting Information), the uptake of 46 water molecules may be involved in formation of the folate monomer from the folate dimer. However, because ~100 water molecules are predicted to be lost upon formation of the EcDHFR·DHF complex, these calculations indicate a net loss of water. In addition, various estimates of the *E. coli* cytosolic DHF concentration range from 50 μM[96] to 300 μM.[20] As these values are much lower than the dimer K_d, they suggest a contribution from the folate dimer model may be minimal unless the presence of osmolytes greatly alters the K_d value.

A second model for explaining water uptake uses a variation of the preferential interaction model in which the osmolytes bind to DHF, albeit weakly. As shown in Figure 6, both osmolyte and water must be released for DHF to bind to EcDHFR. If osmolytes are bound specifically and are more difficult to release than water, then weaker binding of substrate to DHFR results. In this scenario, the osmolytes inhibit complex formation. A corollary of this model is that if a weak interaction occurs between the osmolytes and DHF and/or folate, then perhaps folate and/or DHF may bind to various proteins and/or cellular components. Some support for this corollary comes from various examples of nonspecific folate binding to proteins[97−99] as well as specific binding of folate to the central cavity in hemoglobin.[100] Also, the Record group has experimentally found that betaine can compete with water and interact with amide and cationic nitrogens as well as aromatic hydrocarbons in small molecules.[101] Because folate possesses some of these motifs, this is additional support for the notion that betaine can interact directly with folate. These models are now being probed by experiments in our lab.

Another avenue for addressing the model shown in Figure 6 is to ask about the mechanism by which osmolytes affect K_d values and whether the osmolytes affect k_{on} and/or k_{off} rates. Stopped flow experiments confirmed the effects of betaine on DHF and cofactor binding seen in the ITC studies. Decreases in k_{off} were noted for both ligands, as well as a decrease in k_{on} for DHF binding.

In our study with EcDHFR, an increased affinity of the cofactor for the enzyme in 20 and 0% betaine indicates that water is released upon binding. Thus, it was not surprising that k_{off} decreased for the cofactor bound to the enzyme when the buffer contained betaine. This would correspond to water uptake upon dissociation of the protein−ligand complex. The k_{off} rate also decreased for DHF binding in 20% betaine, albeit to a lesser extent than for the cofactor. This result is consistent with water uptake upon DHF release and correlates with the calculated changes in the accessible surface area (see the Supporting Information) as well as the model presented in Figure 6.

The decrease in the affinity for DHF from ITC experiments appears most correlated with the decrease in the on rate constant in the presence of betaine. With a 6-fold decrease in k_{on} in 20% betaine, compared to 0% betaine, and only a slight (<50%) decrease in k_{off}, betaine appears to be hindering the binding of DHF to the enzyme. This result, coupled with similar Δn_w values for R67 DHFR and EcDHFR, supports our model in Figure 6 in which betaine exerts its effect on free DHF. The decrease in both k_{on} and k_{off} in the presence of betaine suggests that betaine may be affecting DHF binding in multiple ways.

Thermodynamic Cycle Analysis. The free energies, enthalpies, and entropies for the thermodynamic binding cycle in MTA buffer are shown in Figure 7. The free energies are close to being additive. The <1 kcal/mol discrepancy for ΔG may arise from our fitting process which treats a ternary binding event as a binary one; i.e., fitting to a single-site model assumes no enthalpic contributions occur due to formation of the enzyme·first ligand complex. However, closer inspection of the thermodynamic cycle indicates the enthalpies are not close to being additive. Because both ΔG and ΔH are state functions, they should be additive (see, for example, ref 102).

While the analysis described above considers $\Delta H_{observed}$, a similar discrepancy occurs when $\Delta H_{binding}$ is considered (see Table 2). For DHF, the values for binary and ternary complex formation are within error of each other. In contrast, there is an ~10 kcal/mol difference between binary and ternary $NADP^+$ binding events. This enthalpic difference probably does not report on either protonation or solvation differences as the data in Tables 2 and 3 suggest similar protonation and Δn_w effects.

Conclusions. Our ITC studies find addition of osmolytes weakens binding of DHF to both EcDHFR and R67 DHFR.[8] The commonality of these results suggests that at high concentrations, osmolytes can interact with DHF and/or folate and impede binding. This hypothesis is additionally supported by our stopped flow analysis of binding of DHF to EcDHFR in the presence of betaine, where k_{on} rates are clearly affected. As our in vitro results indicate that water uptake or release affects K_d values, one question that arises is what happens in the crowded conditions of the cell. For example, do our osmotic stress studies have any physiological implications? Support for in vivo effects comes from our previous study of R67 DHFR where sensitivity to water activity was probed by addition of increasing concentrations of sorbitol to minimal medium in the

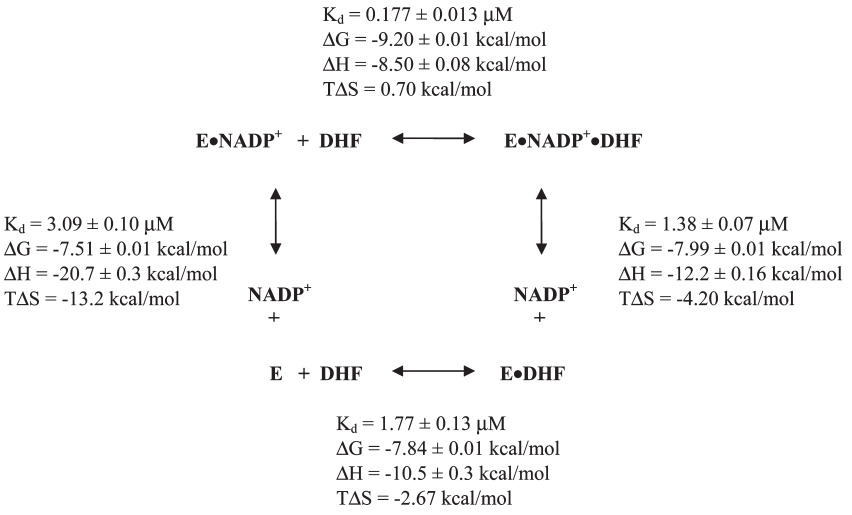

Figure 7. Thermodynamic cycle describing formation of binary and ternary complexes in MTA buffer (pH 7) with the corresponding ITC values. The ΔG values were calculated from the relationship $\Delta G = -RT \ln K_d$, while the $T\Delta S$ values were obtained from the relationship $\Delta G = \Delta H - T\Delta S$. $\Delta H_{observed}$ values are listed.

presence of the antibacterial drug trimethoprim.[8] The ability of the wild type and mutant clones of R67 DHFR to allow host *E. coli* to grow in the presence of trimethoprim and added sorbitol paralleled the catalytic efficiency of the DHFR species, indicating water content (or conversely osmolyte concentration) strongly correlated with the in vivo function of R67 DHFR.

On the basis of the correlation described above, it is interesting to speculate that alteration of in vivo water activity could modulate DHF binding and thus catalysis at low substrate concentrations. Also, Fierke et al. found that the rate of release of THF from the EcDHFR·THF complex is 1.4 s^{-1}, which is much slower than the steady state rate of 12 s^{-1}. Fierke et al. proposed a complicated scheme in which the release of THF from the enzyme·$NADP^+$·THF product complex is facilitated by the initial loss of $NADP^+$ followed by addition of NADPH to form the EcDHFR·THF·NADPH complex. The rate of release of THF from this complex is much faster, i.e., 12.5 s^{-1}. If THF release rates are also modulated by water activity, this could impact the rate-determining step in EcDHFR.[38] Another pertinent question is which elements of the folate structure result in modulation of K_d values by water activity. Depending on the answer, these results could also influence the binding of folate metabolites to other folate pathway enzymes. It also might potentially modulate the effectiveness of folate-based drugs.

■ ASSOCIATED CONTENT

Supporting Information. ITC fit values (six tables), a figure showing the raw ITC data for the $NADP^+$ binary titration (the corresponding Origin fit and a global SEDPHAT fit with a second data set are shown), graphs of ln $K_{a(DHF)}$ versus solution dielectric and ln $K_{a(NADPH)}$ versus osmolality, CD spectra of apo DHFR in the presence of osmolytes as well as an enthalpy−entropy compensation plot, a figure and a table showing the relationship between ln molar volume (V_{mol}) and slope or Δn_w, sample stopped flow data, and a discussion of changes in accessible surface area. This material is available free of charge via the Internet at http://pubs.acs.org.

■ AUTHOR INFORMATION

Corresponding Author

*Department of Biochemistry and Cellular and Molecular Biology, University of Tennessee, Knoxville, TN 37996-0840. Phone: (865) 974-4507. Fax: (865) 974-6306. E-mail: lzh@utk.edu.

Funding Sources

This work was supported by National Science Foundation Grant MCB-0817827.

■ ACKNOWLEDGMENT

We thank Donald Rau [National Institutes of Health (NIH), Bethesda, MD] for suggesting we focus on free DHF. We additionally thank Peter Schuck (NIH), Chris Stanley (Oak Ridge National Laboratories, Oak Ridge, TN), Mike Fried (University of Kentucky, Lexington, KY), Engin Serpersu, and Peter Mazur for helpful discussions. We thank Dan Roberts for the use of his stopped flow. We dedicate this manuscript to the memory of Chetan Padmashali, who initiated these experiments but died in February 2009.

■ ABBREVIATIONS

EcDHFR, *E. coli* dihydrofolate reductase; DHF, dihydrofolate; THF, tetrahydrofolate; NADPH and $NADPH^+$, reduced and oxidized forms of nicotinamide adenine dinucleotide phosphate, respectively; MTX, methotrexate; ITC, isothermal titration calorimetry; wt, wild type; MTA buffer, 100 mM Tris, 50 mM MES, and 50 mM acetic acid polybuffer; SID buffer, 33 mM succinic acid, 44 mM imidazole, and 44 mM diethanolamine polybuffer; E, enzyme; TMAO, trimethylamine oxide; DMSO, dimethyl sulfoxide; PEG, polyethylene glycol; V_{mol}, molar volume; ASA, solvent accessible surface area; ν_{H_2O} and ν_S, stoichiometric coefficients of water and osmolyte, respectively; Δn_w, number of waters taken up or released upon binding; PDB, Protein Data Bank.

REFERENCES

(1) Schnell, J. R., Dyson, H. J., and Wright, P. E. (2004)Structure, dynamics, and catalytic function of dihydrofolate reductase. *Annu. Rev. Biophys. Biomol. Struct. 33*, 119–140.

(2) Rajagopalan, P. T., and Benkovic, S. J. (2002)Preorganization and protein dynamics in enzyme catalysis. *Chem. Rec. 2*, 24–36.

(3) Sawaya, M. R., and Kraut, J. (1997)Loop and subdomain movements in the mechanism of *Escherichia coli* dihydrofolate reductase: Crystallographic evidence. *Biochemistry 36*, 586–603.

(4) Subramanian, S., and Kaufman, B. T. (1978)Interaction of methotrexate, folates, and pyridine nucleotides with dihydrofolate reductase: Calorimetric and spectroscopic binding studies. *Proc. Natl. Acad. Sci. U.S.A. 75*, 3201–3205.

(5) Gilli, R. M., Sari, J. C., Sica, L. M., and Briand, C. M. (1988) Thermodynamic study of the influence of NADPH on the binding of methotrexate and its metabolites to a mammalian dihydrofolate reductase. *Biochim. Biophys. Acta 964*, 53–60.

(6) Sica, L., Gilli, R., Briand, C., and Sari, J. C. (1987)A flow microcalorimetric method for enzyme activity measurements: Application to dihydrofolate reductase. *Anal. Biochem. 165*, 341–348.

(7) Todd, M. J., and Gomez, J. (2001)Enzyme kinetics determined using calorimetry: A general assay for enzyme activity? *Anal. Biochem. 296*, 179–187.

(8) Chopra, S., Dooling, R., Horner, C. G., and Howell, E. E. (2008) A balancing act: Net uptake of water during dihydrofolate binding and net release of water upon NADPH binding in R67 dihydrofolate reductase. *J. Biol. Chem. 283*, 4690–4698.

(9) Bolin, J., Filman, D., Matthews, D., Hamlin, R., and Kraut, J. (1982)Crystal structures of *Escherichia coli* and *Lactobacillus casei* dihydrofolate reductase refined at 1.7 Å resolution. I. General features and binding of methotrexate. *J. Biol. Chem. 257*, 13650.

(10) Bystroff, C., and Kraut, J. (1991)Crystal structure of unliganded *Escherichia coli* dihydrofolate reductase. Ligand-induced conformational changes and cooperativity in binding. *Biochemistry 30*, 2227–2239.

(11) Boehr, D. D., McElheny, D., Dyson, H. J., and Wright, P. E. (2006)The dynamic energy landscape of dihydrofolate reductase catalysis. *Science 313*, 1638–1642.

(12) Boehr, D. D., McElheny, D., Dyson, H. J., and Wright, P. E. (2010)Millisecond timescale fluctuations in dihydrofolate reductase are exquisitely sensitive to the bound ligands. *Proc. Natl. Acad. Sci. U.S.A. 107*, 1373–1378.

(13) Venkitakrishnan, R. P., Zaborowski, E., McElheny, D., Benkovic, S. J., Dyson, H. J., and Wright, P. E. (2004)Conformational changes in the active site loops of dihydrofolate reductase during the catalytic cycle. *Biochemistry 43*, 16046–16055.

(14) Bradrick, T. D., Beechem, J. M., and Howell, E. E. (1996) Unusual binding stoichiometries and cooperativity are observed during binary and ternary complex formation in the single active pore of R67 dihydrofolate reductase, a D_2 symmetric protein. *Biochemistry 35*, 11414–11424.

(15) Park, H., Bradrick, T. D., and Howell, E. E. (1997)A glutamine 67 to histidine mutation in homotetrameric R67 dihydrofolate reductase results in four mutations per single active site pore and causes substantial substrate and cofactor inhibition. *Protein Eng., Des. Sel. 10*, 1415–1424.

(16) Pitcher, W. H., III, DeRose, E. F., Mueller, G. A., Howell, E. E., and London, R. E. (2003)NMR studies of the interaction of a type II dihydrofolate reductase with pyridine nucleotides reveal unexpected phosphatase and reductase activity. *Biochemistry 42*, 11150–11160.

(17) Krahn, J., Jackson, M., DeRose, E. F., Howell, E. E., and London, R. E. (2007)Structure of a type II dihydrofolate reductase ternary complex: Use of identical binding sites for unrelated ligands. *Biochemistry 46*, 14878–14888.

(18) Narayana, N., Matthews, D. A., Howell, E. E., and Nguyen-huu, X. (1995)A plasmid-encoded dihydrofolate reductase from trimethoprim-resistant bacteria has a novel D2-symmetric active site. *Nat. Struct. Biol. 2*, 1018–1025.

(19) Howell, E. E. (2005)Searching sequence space: Two different approaches to dihydrofolate reductase catalysis. *ChemBioChem 6*, 590–600.

(20) Fierke, C. A., Kuchta, R. D., Johnson, K. A., and Benkovic, S. J. (1987)Implications for enzymic catalysis from free-energy reaction coordinate profiles. *Cold Spring Harbor Symp. Quant. Biol. 52*, 631–638.

(21) Alonso, H., and Gready, J. E. (2006)Integron-sequestered dihydrofolate reductase: A recently redeployed enzyme. *Trends Microbiol. 14*, 236–242.

(22) Yahashiri, A., Howell, E. E., and Kohen, A. (2008)Tuning of the H-Transfer Coordinate in Primitive versus Well-Evolved Enzymes. *ChemPhysChem 9*, 980–982.

(23) Fried, M. G., Stickle, D. F., Smirnakis, K. V., Adams, C., MacDonald, D., and Lu, P. (2002)Role of hydration in the binding of lac repressor to DNA. *J. Biol. Chem. 277*, 50676–50682.

(24) Arakawa, T., and Timasheff, S. N. (1985)The stabilization of proteins by osmolytes. *Biophys. J. 47*, 411–414.

(25) Timasheff, S. N. (1993)The control of protein stability and association by weak interactions with water: How do solvents affect these processes? *Annu. Rev. Biophys. Biomol. Struct. 22*, 67–97.

(26) Street, T. O., Bolen, D. W., and Rose, G. D. (2006)A molecular mechanism for osmolyte-induced protein stability. *Proc. Natl. Acad. Sci. U.S.A. 103*, 13997–14002.

(27) Reid, C., and Rand, R. P. (1997)Probing protein hydration and conformational states in solution. *Biophys. J. 72*, 1022–1030.

(28) LiCata, V. J., and Allewell, N. M. (1997)Functionally linked hydration changes in *Escherichia coli* aspartate transcarbamylase and its catalytic subunit. *Biochemistry 36*, 10161–10167.

(29) Flensburg, J., and Skold, O. (1987)Massive overproduction of dihydrofolate reductase in bacteria as a response to the use of trimethoprim. *Eur. J. Biochem. 162*, 473–476.

(30) Baccanari, D. P., Stone, D., and Kuyper, L. (1981)Effect of a single amino acid substitution on *Escherichia coli* dihydrofolate reductase catalysis and ligand binding. *J. Biol. Chem. 256*, 1738–1747.

(31) Ellis, K. J., and Morrison, J. F. (1982)Buffers of constant ionic strength for studying pH-dependent processes. *Methods Enzymol. 87*, 405–426.

(32) Wiseman, T., Williston, S., Brandts, J. F., and Lin, L. N. (1989) Rapid measurement of binding constants and heats of binding using a new titration calorimeter. *Anal. Biochem. 179*, 131–137.

(33) Houtman, J. C., Brown, P. H., Bowden, B., Yamaguchi, H., Appella, E., Samelson, L. E., and Schuck, P. (2007)Studying multisite binary and ternary protein interactions by global analysis of isothermal titration calorimetry data in SEDPHAT: Application to adaptor protein complexes in cell signaling. *Protein Sci. 16*, 30–42.

(34) Fukada, H., and Takahashi, K. (1998)Enthalpy and heat capacity changes for the proton dissociation of various buffer components in 0.1 M potassium chloride. *Proteins 33*, 159–166.

(35) Jelesarov, I., and Bosshard, H. R. (1994)Thermodynamics of ferredoxin binding to ferredoxin:$NADP^+$ reductase and the role of water at the complex interface. *Biochemistry 33*, 13321–13328.

(36) Sweeney, T. E., and Beuchat, C. A. (1993)Limitations of methods of osmometry: Measuring the osmolality of biological fluids. *Am. J. Physiol. 264*, R469–R480.

(37) Wyman, J., Jr. (1964)Linked functions and reciprocal effects in hemoglobin: A second look. *Adv. Protein Chem. 19*, 223–286.

(38) Fierke, C. A., Johnson, K. A., and Benkovic, S. J. (1987) Construction and evaluation of the kinetic scheme associated with dihydrofolate reductase from *Escherichia coli*. *Biochemistry 26*, 4085–4092.

(39) Maharaj, G., Selinsky, B. S., Appleman, J. R., Perlman, M., London, R. E., and Blakley, R. L. (1990)Dissociation constants for dihydrofolic acid and dihydrobiopterin and implications for mechanistic models for dihydrofolate reductase. *Biochemistry 29*, 4554–4560.

(40) Cayley, P. J., Dunn, S. M., and King, R. W. (1981)Kinetics of substrate, coenzyme, and inhibitor binding to *Escherichia coli* dihydrofolate reductase. *Biochemistry 20*, 874–879.

(41) Fersht, A. (1999) *Structure and Mechanism in Protein Science*, W. H. Freeman and Co., New York.
(42) Posner, B. A., Li, L., Bethell, R., Tsuji, T., and Benkovic, S. J. (1996)Engineering specificity for folate into dihydrofolate reductase from *Escherichia coli*. *Biochemistry 35*, 1653–1663.
(43) Chen, Y. Q., Kraut, J., Blakley, R. L., and Callender, R. (1994) Determination by Raman spectroscopy of the pK_a of N5 of dihydrofolate bound to dihydrofolate reductase: Mechanistic implications. *Biochemistry 33*, 7021–7026.
(44) Deng, H., and Callender, R. (1998)Structure of dihydrofolate when bound to DHFR. *J. Am. Chem. Soc. 120*, 7730–7737.
(45) Cannon, W., Garrison, B., and Benkovic, S. (1997)Electrostatic characterization of enzyme complexes: Evaluation of the mechanism of catalysis of dihydrofolate reductase. *J. Am. Chem. Soc. 119*, 2386–2395.
(46) Rod, T. H., and Brooks, C. L., III (2003)How dihydrofolate reductase facilitates protonation of dihydrofolate. *J. Am. Chem. Soc. 125*, 8718–8719.
(47) Ferrer, S., Silla, E., Tunon, I., Marti, S., and Moliner, V. (2003) Catalytic mechanism of dihydrofolate reductase enzyme. A combined quantum mechanical/molecular-mechanical characterization of the N5 protonation step. *J. Phys. Chem. B 107*, 14036–14041.
(48) Shrimpton, P., and Allemann, R. K. (2002)Role of water in the catalytic cycle of *E. coli* dihydrofolate reductase. *Protein Sci. 11*, 1442–1451.
(49) Chen, Y. Q., Kraut, J., and Callender, R. (1997)pH-dependent conformational changes in *Escherichia coli* dihydrofolate reductase revealed by Raman difference spectroscopy. *Biophys. J. 72*, 936–941.
(50) Cummins, P. L., and Gready, J. E. (2001)Energetically most likely substrate and active-site protonation sites and pathways in the catalytic mechanism of dihydrofolate reductase. *J. Am. Chem. Soc. 123*, 3418–3428.
(51) Feeney, J., Birdsall, B., Roberts, G. C., and Burgen, A. S. V. (1975)^{31}P NMR studies of NADPH and $NADP^+$ binding to *L. casei* dihydrofolate reductase. *Nature 257*, 564–566.
(52) Parsegian, V. A., Rand, R. P., and Rau, D. C. (1995)Macromolecules and water: Probing with osmotic stress. *Methods Enzymol. 259*, 43–94.
(53) LiCata, V. J., and Allewell, N. M. (1998)Measuring hydration changes of proteins in solution: Applications of osmotic stress and structure-based calculations. *Methods Enzymol. 295*, 42–62.
(54) Robinson, C. R., and Sligar, S. G. (1995)Hydrostatic and osmotic pressure as tools to study macromolecular recognition. *Methods Enzymol. 259*, 395–427.
(55) Kornblatt, J. A., and Kornblatt, M. J. (2002)The effects of osmotic and hydrostatic pressures on macromolecular systems. *Biochim. Biophys. Acta 1595*, 30–47.
(56) Edsall, J. (1943) Dielectric constants and dipole moments of dipolar ions. In *Proteins, Amino Acids and Peptides as Ions and Dipolar Ions* (Cohn, E., and Edsall, J., Eds.) pp 140−154, Reinhold, New York.
(57) Kiser, J. R., Monk, R. W., Smalls, R. L., and Petty, J. T. (2005) Hydration changes in the association of Hoechst 33258 with DNA. *Biochemistry 44*, 16988–16997.
(58) Timasheff, S. N. (2002)Protein-solvent preferential interactions, protein hydration, and the modulation of biochemical reactions by solvent components. *Proc. Natl. Acad. Sci. U.S.A. 99*, 9721–9726.
(59) Parsegian, V. A., Rand, R. P., and Rau, D. C. (2000)Osmotic stress, crowding, preferential hydration, and binding: A comparison of perspectives. *Proc. Natl. Acad. Sci. U.S.A. 97*, 3987–3992.
(60) Vossen, K. M., Wolz, R., Daugherty, M. A., and Fried, M. G. (1997) Role of macromolecular hydration in the binding of the *Escherichia coli* cyclic AMP receptor to DNA. *Biochemistry 36*, 11640–11647.
(61) Sidorova, N. Y., Muradymov, S., and Rau, D. C. (2006) Differences in hydration coupled to specific and nonspecific competitive binding and to specific DNA binding of the restriction endonuclease BamHI. *J. Biol. Chem. 281*, 35656–35666.
(62) Courtenay, E. S., Capp, M. W., Anderson, C. F., and Record, M. T., Jr. (2000)Vapor pressure osmometry studies of osmolyte-protein interactions: Implications for the action of osmoprotectants in vivo and for the interpretation of "osmotic stress" experiments in vitro. *Biochemistry 39*, 4455–4471.
(63) Schellman, J. A. (2003)Protein stability in mixed solvents: A balance of contact interaction and excluded volume. *Biophys. J. 85*, 108–125.
(64) Schurr, J. M., Rangel, D. P., and Aragon, S. R. (2005)A contribution to the theory of preferential interaction coefficients. *Biophys. J. 89*, 2258–2276.
(65) Minton, A. P. (1981)Excluded volume as a determinant of macromolecular structure and reactivity. *Biopolymers 20*, 2093–2120.
(66) Garner, M. M., and Rau, D. C. (1995)Water release associated with specific binding of gal repressor. *EMBO J. 14*, 1257–1263.
(67) Sidorova, N., and Rau, D. C. (2004)The role of water in the EcoRI-DNA binding. *Nucleic Acids Mol. Biol. 14*, 319–337.
(68) Hultgren, A., and Rau, D. C. (2004)Exclusion of alcohols from spermidine-DNA assemblies: Probing the physical basis of preferential hydration. *Biochemistry 43*, 8272–8280.
(69) Davis-Searles, P. R., Morar, A. S., Saunders, A. J., Erie, D. A., and Pielak, G. J. (1998)Sugar-induced molten-globule model. *Biochemistry 37*, 17048–17053.
(70) Saunders, A. J., Davis-Searles, P. R., Allen, D. L., Pielak, G. J., and Erie, D. A. (2000)Osmolyte-induced changes in protein conformational equilibria. *Biopolymers 53*, 293–307.
(71) Gulotta, M., Qiu, L., Desamero, R., Rosgen, J., Bolen, D. W., and Callender, R. (2007)Effects of cell volume regulating osmolytes on glycerol 3-phosphate binding to triosephosphate isomerase. *Biochemistry 46*, 10055–10062.
(72) Auton, M., and Bolen, D. W. (2005)Predicting the energetics of osmolyte-induced protein folding/unfolding. *Proc. Natl. Acad. Sci. U.S.A. 102*, 15065–15068.
(73) Chik, J., Mizrahi, S., Chi, S., Parsegian, V. A., and Rau, D. C. (2005)Hydration forces underlie the exclusion of salts and of neutral polar solutes from hydroxypropylcellulose. *J. Phys. Chem. B 109*, 9111–9118.
(74) Stanley, C., and Rau, D. C. (2006)Preferential hydration of DNA: The magnitude and distance dependence of alcohol and polyol interactions. *Biophys. J. 91*, 912–920.
(75) Chervenak, M. C. T., and Eric, J. (1994)A direct measure of the contribution of solvent reorganization to the enthalpy of binding. *J. Am. Chem. Soc. 116*, 10533–10539.
(76) Dunitz, J. D. (1995)Win some, lose some: Enthalpy-entropy compensation in weak intermolecular interactions. *Chem. Biol. 2*, 709–712.
(77) Frisch, C., Schreiber, G., Johnson, C. M., and Fersht, A. R. (1997)Thermodynamics of the interaction of barnase and barstar: Changes in free energy versus changes in enthalpy on mutation. *J. Mol. Biol. 267*, 696–706.
(78) Harries, D., Rau, D. C., and Parsegian, V. A. (2005)Solutes probe hydration in specific association of cyclodextrin and adamantane. *J. Am. Chem. Soc. 127*, 2184–2190.
(79) Dunn, S. M., Lanigan, T. M., and Howell, E. E. (1990) Dihydrofolate reductase from *Escherichia coli*: Probing the role of aspartate-27 and phenylalanine-137 in enzyme conformation and the binding of NADPH. *Biochemistry 29*, 8569–8576.
(80) Appleman, J. R., Howell, E. E., Kraut, J., and Blakley, R. L. (1990)Role of aspartate 27 of dihydrofolate reductase from *Escherichia coli* in interconversion of active and inactive enzyme conformers and binding of NADPH. *J. Biol. Chem. 265*, 5579–5584.
(81) Adams, J., Johnson, K. A., Matthews, C. R., and Benkovic, S. J. (1989)Effects of distal point-site mutations on the binding and catalysis of dihydrofolate reductase from *Escherichia coli*. *Biochemistry 28*, 6611–6618.
(82) Loveridge, E. J., Tey, L. H., and Allemann, R. K. (2010)Solvent effects on catalysis by *Escherichia coli* dihydrofolate reductase. *J. Am. Chem. Soc. 132*, 1137–1143.
(83) Jackson, M., Chopra, S., Smiley, R. D., Maynord, P. O., Rosowsky, A., London, R. E., Levy, L., Kalman, T. I., and Howell, E. E. (2005)Calorimetric studies of ligand binding in R67 dihydrofolate reductase. *Biochemistry 44*, 12420–12433.

(84) Ortiz-Salmeron, E., Yassin, Z., Clemente-Jimenez, M. J., Las Heras-Vazquez, F. J., Rodriguez-Vico, F., Baron, C., and Garcia-Fuentes, L. (2001)Thermodynamic analysis of the binding of glutathione to glutathione S-transferase over a range of temperatures. *Eur. J. Biochem. 268*, 4307–4314.

(85) Miyagi, M., Wan, Q., Ahmad, M. F., Gokulrangan, G., Tomechko, S. E., Bennett, B., and Dealwis, C. (2011)Histidine hydrogen-deuterium exchange mass spectrometry for probing the microenvironment of histidine residues in dihydrofolate reductase. *PLoS One 6*, e17055.

(86) Appleman, J. R., Howell, E. E., Kraut, J., Kuhl, M., and Blakley, R. L. (1988)Role of aspartate 27 in the binding of methotrexate to dihydrofolate reductase from *Escherichia coli*. *J. Biol. Chem. 263*, 9187–9198.

(87) Boehr, D. D., Dyson, H. J., and Wright, P. E. (2006)An NMR perspective on enzyme dynamics. *Chem. Rev. 106*, 3055–3079.

(88) Boehr, D. D., Dyson, H. J., and Wright, P. E. (2008)Conformational relaxation following hydride transfer plays a limiting role in dihydrofolate reductase catalysis. *Biochemistry 47*, 9227–9233.

(89) Heaslet, H., Harris, M., Fahnoe, K., Sarver, R., Putz, H., Chang, J., Subramanyam, C., Barreiro, G., and Miller, J. R. (2009)Structural comparison of chromosomal and exogenous dihydrofolate reductase from *Staphylococcus aureus* in complex with the potent inhibitor trimethoprim. *Proteins 76*, 706–717.

(90) Cody, V., Pace, J., and Rosowsky, A. (2008)Structural analysis of a holoenzyme complex of mouse dihydrofolate reductase with NADPH and a ternary complex with the potent and selective inhibitor 2,4-diamino-6-(2′-hydroxydibenz[b,f]azepin-5-yl)methylpteridine. *Acta Crystallogr. D64*, 977–984.

(91) Dzingeleski, G. D., and Wolfenden, R. (1993)Hypersensitivity of an enzyme reaction to solvent water. *Biochemistry 32*, 9143–9147.

(92) Furukawa, Y., and Morishima, I. (2001)The role of water molecules in the association of cytochrome P450cam with putidaredoxin. An osmotic pressure study. *J. Biol. Chem. 276*, 12983–12990.

(93) Xavier, K. A., Shick, K. A., Smith-Gil, S. J., and Willson, R. C. (1997) Involvement of water molecules in the association of monoclonal antibody HyHEL-5 with bobwhite quail lysozyme. *Biophys. J. 73*, 2116–2125.

(94) Poe, M. (1973)Proton magnetic resonance studies of folate, dihydrofolate, and methotrexate. Evidence from pH and concentration studies for dimerization. *J. Biol. Chem. 248*, 7025–7032.

(95) Carlson, J. C., Kanter, A., Thuduppathy, G. R., Cody, V., Pineda, P. E., McIvor, R. S., and Wagner, C. R. (2003)Designing protein dimerizers: The importance of ligand conformational equilibria. *J. Am. Chem. Soc. 125*, 1501–1507.

(96) Lu, W., Kwon, Y. K., and Rabinowitz, J. D. (2007)Isotope ratio-based profiling of microbial folates. *J. Am. Soc. Mass Spectrom. 18*, 898–909.

(97) Fernandes-Costa, F., and Metz, J. (1979)Role of serum folate binders in the delivery of folate to tissues and to the fetus. *Br. J. Haematol. 41*, 335–342.

(98) De Wit, R., and Bulgakov, R. (1985)Guanine nucleotides modulate the ligand binding properties of cell surface folate receptors in *Dictyostelium discoideum*. *FEBS Lett. 179*, 257–261.

(99) Corrocher, R., De Sandre, G., Ambrosetti, A., Pachor, M. L., Bambara, L. M., and Hoffbrand, A. V. (1978)Specific and non-specific folate binding protein in normal and malignant human tissues. *J. Clin. Pathol. 31*, 659–665.

(100) Arnone, A., Rogers, P. H., Benesch, R. E., Benesch, R., and Kwong, S. (1986)The interaction of folylpolyglutamates with deoxyhemoglobin. Identification of the binding site. *J. Biol. Chem. 261*, 5853–5857.

(101) Capp, M. W., Pegram, L. M., Saecker, R. M., Kratz, M., Riccardi, D., Wendorff, T., Cannon, J. G., and Record, M. T., Jr. (2009)Interactions of the osmolyte glycine betaine with molecular surfaces in water: Thermodynamics, structural interpretation, and prediction of m-values. *Biochemistry 48*, 10372–10379.

(102) Norris, A. L., and Serpersu, E. (2010)Interactions of coenzyme A with the aminoglycoside acetyltransferase (3)-IIIb and thermodynamics of a ternary system. *Biochemistry 49*, 4036–4042.